

# The Datta-Das transistor: Significance of channel direction, size-dependence of source contacts, and boundary effects

Ming-Hao Liu and Ching-Ray Chang

Department of Physics, National Taiwan University, Taipei 106, Taiwan

(Date textdate)

We analyze the spin expectation values for injected spin-polarized electrons in a [001]-grown inversion-asymmetric two-dimensional electron gas (2DEG), where both Rashba and Dresselhaus spin-orbit couplings are taken into account. Based on the single-point spin injection, we obtain the most general formulae for the spin vectors in such Rashba-Dresselhaus type 2DEGs and show the significance of channel direction for the Datta-Das transistor. Extension to spin injection via a finite-sized source contact is introduced, and the change thus induced is found to be moderate. Exploiting the plane wave property of the electron in the 2DEG, we proposed a simplified model to examine possible effects due to the channel boundary. We find that such influences are due to the channel boundary effect and the finite size of the spin injection source contact becomes weak when the spin-splitting strength is strong. Hence we conclude that [110] is a robust channel direction and is therefore the best candidate for the design of the Datta-Das transistor.

PACS numbers: 72.25.Dc, 71.70.Ej, 85.75.Hh

## I. INTRODUCTION

The Datta-Das spin-field-effect transistor (spin-FET),<sup>1</sup> stimulating plenty of both theoretical and experimental works in semiconductor spintronics,<sup>2</sup> has not yet been realized. Concluded difficulties are basically:<sup>3</sup> (i) effective controllability of the Rashba spin-orbit<sup>4</sup> (SO) coupling strength  $\alpha$ , (ii) long spin-relaxation time in two-dimensional electron gas (2DEG) systems, (iii) uniformity of  $\alpha$ , and (iv) more efficient spin injection rate. So far, the former two conditions have been basically satisfied in experiments,<sup>7,8</sup> while the latter two remain to be solved.

Whereas the Datta-Das transistor is designed to use a Rashba-type 2DEG channel, the structure inversion asymmetry (the Rashba SO term) is required to dominate over the bulk inversion asymmetry (the Dresselhaus SO term,<sup>9</sup> with coupling strength  $\beta$ ) therein. However, the coupling strengths of the Rashba and Dresselhaus terms have been, in fact, found to be of the same order in certain types of quantum wells.<sup>5,6</sup> Therefore, the influence due to the Dresselhaus term in the Datta-Das transistor has become another attractive topic in spintronics. For example, it was Łusakowski *et al.*, who showed that the conductance of the Datta-Das spin-FET depends significantly on the crystallographic direction of the channel when the Dresselhaus term is also present.<sup>10</sup> A more complete work done by Winkler is the investigation of the spin-splitting due to the effective magnetic field generated by the structure inversion asymmetry and the bulk inversion asymmetry.<sup>11,12</sup> Very recently, our previous work following Winkler even derived the analytical formulae of the electron spin precession in the 2DEG with both the Rashba and Dresselhaus terms involved.<sup>13</sup>

The formulae obtained in Ref.<sup>13</sup> also implies the significance of the 2DEG channel direction, and is therefore in correspondence with Łusakowski's result. However, the assumption of spin injection via an ideal point contact and the neglect of boundary effects in the 2DEG channel need be further investigated. In this paper, we mainly extend our previous work<sup>13</sup> to include spin injection via a finite-sized source

contact and to take the boundary effect into account. The former consideration is found to provide an average effect and the change thus induced is therefore moderate, while the latter may bring drastic influences. Both effects are concluded to be inversely proportional to the SO strength. In the case of  $\alpha\beta > 0$ , i.e., the Rashba and Dresselhaus SO couplings are of the same sign, electrons encounter the strongest spin-splitting along the [110] direction,<sup>14</sup> which is therefore concluded to be a robust channel direction as a good choice of the Datta-Das spin-FET.

This paper is organized as follows. In Sec. II we introduce our theoretical formalism to compute the spin vectors in the Rashba-Dresselhaus 2DEGs, and construct a model to investigate the effects due to the size of the spin injection source contact and the influence due to the channel boundary. We then present numerical results in Sec. III to show the specific changes due to these further considerations, and conclude with Sec. IV. Throughout this paper, we work within the single-particle picture using a standard quantum mechanical approach and assume zero temperature in the clean limit.

## II. THEORETICAL FORMALISM

To characterize the spin orientation of the electron injected from a ferromagnetic source contact into a Rashba-Dresselhaus type 2DEG, the basic task is to find out the state ket of the injected electron when evolved to an arbitrary space point  $\mathbf{r} = (r, \phi)$  in the 2DEG, and then to evaluate the expectation of the spin operator with respect to this state ket. In this section, we construct a simple formalism to calculate the evolved electron state ket considering finite-sized source contact for spin injection and the boundary effect in the 2DEG channel as well.

### A. Single-point spin injection without channel boundary

We first generalize the formulae obtained in Ref.<sup>13</sup>, which mainly describes the in-plane behavior of the electron spin, injected from an inplane-magnetized ferromagnet into an inversion-asymmetric 2DEG, via an ideal quantum point contact. Referring their results as  $\langle \mathbf{S} \rangle_r^{\parallel}$  with the superscript denoting that the injected spin is inplane-polarized while the subscript is for expectation done on  $\mathbf{r}$ , we are now considering the more general case, namely, ferromagnetic source contacts with arbitrary magnetization. The spinor corresponding to the electron spin injected on  $\mathbf{r}_0$  is therefore written by<sup>15</sup>  $|\mathbf{s}_{\text{inj}}\rangle_{\mathbf{r}_0} \equiv |\tilde{\beta} = \theta_s, \tilde{\alpha} = \phi_s, +\rangle \doteq (e^{i\phi_s} \cos(\theta_s/2), + \sin(\theta_s/2))^{\dagger}$  where  $\tilde{\beta}$  and  $\tilde{\alpha}$  are the polar and azimuthal angles, respectively, and we are thus seeking for the spin vector  $\langle \mathbf{S} \rangle_r = \mathbf{r} \langle \mathbf{s}_{\text{inj}} | \mathbf{S} | \mathbf{s}_{\text{inj}} \rangle_r$ . Also, we present the calculation of  $\langle S_z \rangle_r$  to complete the description of the spatial behavior of the spin vector. Using the same method introduced in Ref.<sup>13</sup>, we obtain, choosing  $\mathbf{r}_0 = \mathbf{0}$ ,

$$\langle \mathbf{S} \rangle_r = \begin{pmatrix} \cos \theta_s \cos \varphi \sin \Delta\theta(\mathbf{r}) + \sin \theta_s \langle S_x \rangle_r^{\parallel} \\ \cos \theta_s \sin \varphi \sin \Delta\theta(\mathbf{r}) + \sin \theta_s \langle S_y \rangle_r^{\parallel} \\ \cos \theta_s \cos \Delta\theta(\mathbf{r}) + \sin \theta_s \langle S_z \rangle_r^{\parallel} \end{pmatrix} \quad (1)$$

with  $\langle S_x \rangle_r^{\parallel}$  and  $\langle S_y \rangle_r^{\parallel}$  given by Eq. (5) of Ref.<sup>13</sup>,  $\langle S_z \rangle_r^{\parallel} = \cos(\varphi - \phi_s) \sin \Delta\theta$ ,  $\varphi \equiv \arg[(\alpha \sin \phi + \beta \cos \phi) + i(\alpha \cos \phi + \beta \sin \phi)]$ , and  $\Delta\theta(\mathbf{r}) = 2m^*r\sqrt{\alpha^2 + \beta^2 + 2\alpha\beta \sin(2\phi)}/\hbar^2$  with  $m^*$  the electron effective mass, for the point spin injection case in the absence of boundary effects. Clearly, Eq. (1) recovers the previous results in Ref.<sup>13</sup> when injecting an inplane-polarized spin, i.e.,  $\langle \mathbf{S} \rangle_r = \langle \mathbf{S} \rangle_r^{\parallel}$  when  $\theta_s = \pi/2$ . Note that in the case of single-point spin injection, the state ket  $|\mathbf{s}_{\text{inj}}\rangle_r$  is given by<sup>13</sup>

$$|\mathbf{s}_{\text{inj}}\rangle_{\mathbf{r}_0 \rightarrow \mathbf{r}} = c_+ e^{-i\frac{\Delta\theta(\mathbf{r}-\mathbf{r}_0)}{2}} |\psi_+\rangle + c_- e^{i\frac{\Delta\theta(\mathbf{r}-\mathbf{r}_0)}{2}} |\psi_-\rangle, \quad (2)$$

where  $|\psi_{\pm}\rangle$  are the eigenspinors of the Rashba-Dresselhaus system and the expansion coefficients are  $c_{\pm} = \langle \psi_{\pm} | \mathbf{s}_{\text{inj}} \rangle_{\mathbf{r}_0}$ . The subscript  $\mathbf{r}_0 \rightarrow \mathbf{r}$  is to remind that the spin is injected on  $\mathbf{r}_0$  and detected on  $\mathbf{r}$  after straight evolution.

### B. Finite-sized spin injection without channel boundary

We now introduce a model to deal with the case of spin injection from a finite-sized source contact, in the framework of single-particle picture. Consider a spin-polarized source connected with the 2DEG channel, either from the side or from the top, via a finite-sized contact. Assume that each electron is equally likely to be injected via all the possible injection points, which may be everywhere of the contact except the positions close to the atoms. Since the electrons are free to move between the atoms, let us assume that the possible injection points locate on exactly the center of each primitive unit cell of the contact crystal for the top injection [see Fig. 1(a), where a simple cubic lattice is used as an example]. In

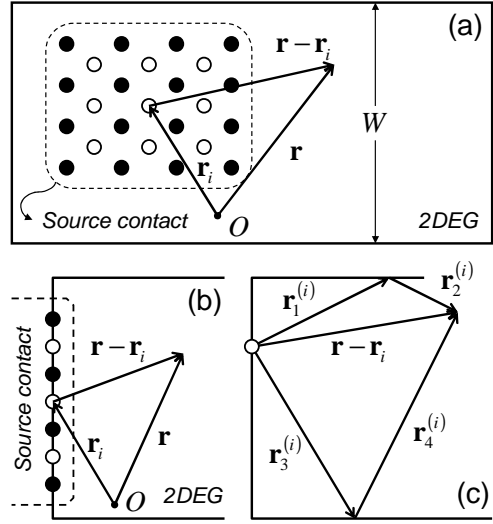


FIG. 1: Top view of the 2DEG channel with spin injection source made by (a) top contact and (b) side contact. Filled and open circles depict atoms and injection points within the contact, respectively. (c) Schematic of propagations of an injected electron in the 2DEG, sketched from the top view.

the case of side injection, the contact region becomes a line and the injection points are reduced to the middle points of each neighboring pair of atoms [Fig. 1(b)]. Note that despite a displacement, the distribution of the injection points are equivalent to the lattice points of the contact.

Let us label the positions of the injection points as  $\mathbf{r}_i$ . Since the electron is equally likely to enter the 2DEG from each injection point, the state ket describing the injected electron detected on  $\mathbf{r}$  can be written as

$$|\mathbf{s}_{\text{inj}}\rangle_r = \frac{1}{\mathbf{r} \langle \mathbf{s}_{\text{inj}} | \mathbf{s}_{\text{inj}} \rangle_r} \sum_i |\mathbf{s}_{\text{inj}}\rangle_{\mathbf{r}_i \rightarrow \mathbf{r}}, \quad (3)$$

where  $|\mathbf{s}_{\text{inj}}\rangle_{\mathbf{r}_i \rightarrow \mathbf{r}}$  is given by (2). Note that this formulation can also include the problem of imperfect spin-polarized injection, i.e., to deal with a multi-domain ferromagnetic source contact. In general, we can write  $|\mathbf{s}_{\text{inj}}\rangle_{\mathbf{r}_i} = |\tilde{\beta} = \theta_s^{(i)}, \tilde{\alpha} = \phi_s^{(i)}, +\rangle$  and obtain each  $|\mathbf{s}_{\text{inj}}\rangle_{\mathbf{r}_i \rightarrow \mathbf{r}} = \sum_{\sigma=\pm} \exp[-i\sigma\Delta\theta(\mathbf{r} - \mathbf{r}_i)/2] \langle \psi_{\sigma} | \mathbf{s}_{\text{inj}} \rangle_{\mathbf{r}_i} |\psi_{\sigma}\rangle$ . In the assumption of perfect polarization, one uses  $|\mathbf{s}_{\text{inj}}\rangle_{\mathbf{r}_i} = |\tilde{\beta} = \theta_s, \tilde{\alpha} = \phi_s, +\rangle$  for all  $\mathbf{r}_i$ .

### C. Finite-sized spin injection with channel boundary

The effect of the lateral confinement in the channel was previously regarded as to provide large energy gap between two neighboring subbands to avoid intersubband mixing in the transverse direction.<sup>1,16,17</sup> Contrary to this suggested quasi-one-dimensional channel, we study two-dimensional propagation and put emphasis on the electron wave property, i.e.,

both longitudinal and transverse directions are not strongly quantized. Based on this view point, we assume that each spin-polarized electron injected on  $\mathbf{r}_i$  may propagate to the detection point  $\mathbf{r}$  through not only the straight but also the reflected paths. The corresponding state ket considering the channel boundary reflection is then written as

$$|\mathbf{s}_{\text{inj}}\rangle_{\mathbf{r}_i \rightarrow \mathbf{r}}^{\text{ref}} = \frac{1}{\langle \mathbf{s}_{\text{inj}} | \mathbf{s}_{\text{inj}} \rangle_{\mathbf{r}_i \rightarrow \mathbf{r}}^{\text{ref}}} \sum_{n=0}^{\infty} |\mathbf{s}_{\text{inj}}\rangle_{\mathbf{r}_i \rightarrow \mathbf{r}}^{(n)}, \quad (4)$$

where  $|\mathbf{s}_{\text{inj}}\rangle_{\mathbf{r}_i \rightarrow \mathbf{r}}^{(n)}$  is the spatially evolved state ket from  $\mathbf{r}_i$  to  $\mathbf{r}$  after  $n$  times of reflection by the channel boundary. To avoid complicating the problem, let us include only the first-order reflection, i.e., we pick terms up to  $n = 1$  in Eq. (4). Thus three paths are considered for each injection and detection pair  $(\mathbf{r}_i \rightarrow \mathbf{r})$ : top reflection  $\mathbf{r}_1^{(i)} \rightarrow \mathbf{r}_2^{(i)}$ , straight  $\mathbf{r} - \mathbf{r}_i$ , and bottom reflection  $\mathbf{r}_3^{(i)} \rightarrow \mathbf{r}_4^{(i)}$ , as illustrated in Fig. 1(c).

Under this construction, the electron unavoidably interferes with itself. For spin injection via  $\mathbf{r}_i$ , the total state ket can be therefore written as

$$|\mathbf{s}_{\text{inj}}\rangle_{\mathbf{r}_i \rightarrow \mathbf{r}}^{\text{ref}} = \frac{1}{\langle \mathbf{s}_{\text{inj}} | \mathbf{s}_{\text{inj}} \rangle_{\mathbf{r}_i \rightarrow \mathbf{r}}^{\text{ref}}} \times \left( |\mathbf{s}_{\text{inj}}\rangle_{\mathbf{r}_i \rightarrow \mathbf{r}} + |\mathbf{s}_{\text{inj}}\rangle_{\mathbf{r}_i \rightarrow \mathbf{r}}^{\text{top}} + |\mathbf{s}_{\text{inj}}\rangle_{\mathbf{r}_i \rightarrow \mathbf{r}}^{\text{bottom}} \right), \quad (5)$$

where the first term corresponds to the straight propagation, i.e., the  $|\mathbf{s}_{\text{inj}}\rangle_{\mathbf{r}_i \rightarrow \mathbf{r}}^{(0)}$  term. Second and third terms corresponding to the  $|\mathbf{s}_{\text{inj}}\rangle_{\mathbf{r}_i \rightarrow \mathbf{r}}^{(1)}$  term describe the reflected waves, and can be obtained by, e.g.,

$$|\mathbf{s}_{\text{inj}}\rangle_{\mathbf{r}_i \rightarrow \mathbf{r}}^{\text{top}} = |\mathbf{s}_{\text{inj}}\rangle_{\mathbf{r}_1^{(i)} \rightarrow \mathbf{r}_2^{(i)}} = \sum_{\sigma=\pm} e^{-i\sigma \frac{\Delta\theta(\mathbf{r}_2^{(i)} - \mathbf{r}_1^{(i)})}{2}} \langle \psi_{\sigma} | \mathbf{s}_{\text{inj}} \rangle_{\mathbf{r}_i \rightarrow \mathbf{r}_1^{(i)}} |\psi_{\sigma}\rangle \quad (6)$$

with

$$|\mathbf{s}_{\text{inj}}\rangle_{\mathbf{r}_i \rightarrow \mathbf{r}_1^{(i)}} = \sum_{\sigma=\pm} e^{-i\sigma \frac{\Delta\theta(\mathbf{r}_1^{(i)} - \mathbf{r}_i)}{2}} \langle \psi_{\sigma} | \mathbf{s}_{\text{inj}} \rangle_{\mathbf{r}_i} |\psi_{\sigma}\rangle. \quad (7)$$

When considering finite-sized injection, the total state ket characterizing the injected electron is expressed as (3), replacing  $|\mathbf{s}_{\text{inj}}\rangle_{\mathbf{r}_i \rightarrow \mathbf{r}} \rightarrow |\mathbf{s}_{\text{inj}}\rangle_{\mathbf{r}_i \rightarrow \mathbf{r}}^{\text{ref}}$  given by (5). Using this space-dependent state ket, one can obtain the spin vectors  $\langle \mathbf{S} \rangle$  everywhere inside the 2DEG channel.

### III. NUMERICAL RESULTS

In this section we present the calculated spin vectors inside the 2DEG channel with certain cases of spin injection, based on the theoretical formalism introduced in the previous section. We show the significance of channel directions in the presence of both Rashba and Dresselhaus SO couplings. In the following two subsections, we investigate InGaAs 2DEGs, setting the Rashba coupling parameter<sup>19</sup>  $\alpha = 0.3 \text{ eV \AA}$  with

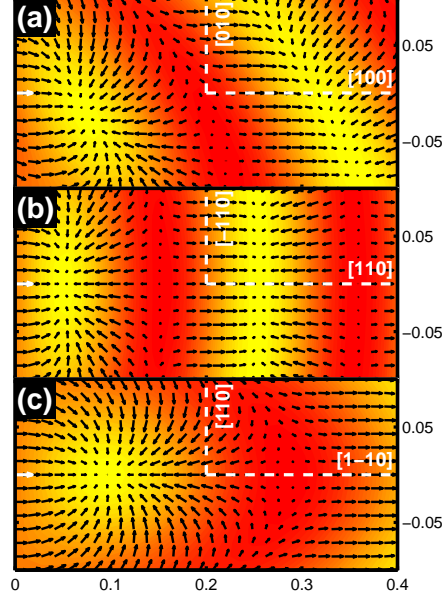


FIG. 2: (Color online) Spin expectations of a spin-polarized electron injected on the middle of the left end (indicated by bold white arrows) for three  $0.4 \mu\text{m} \times 0.2 \mu\text{m}$  channels along (a) [100], (b) [110], and (c) [1 $\bar{1}$ 0]. Color shading is determined by  $\langle S_z \rangle$  with red (dark)  $\rightarrow$  negative and yellow (bright)  $\rightarrow$  positive. All the position labels are in units of  $\mu\text{m}$ .

electron effective mass  $m^* = 0.03m_e$ . The Dresselhaus coupling parameter is chosen as  $\beta = 0.09 \text{ eV \AA}$ , which is deduced from  $\beta \approx \gamma \langle k_z^2 \rangle$  with a typical value for the coefficient<sup>5,20</sup>  $\gamma \approx 25 \text{ eV \AA}^3$ , assuming an infinite quantum well in  $z$ -direction with well width  $50 \text{ \AA}$ . In the last subsection, the values of  $\alpha$  and  $\beta$  are varied and will be mentioned there. Throughout this section, we consider the spin transistor geometry, i.e., injected spin-polarization parallel to the channel direction.

#### A. Significance of channel directions

We begin with the single-point spin injection case for different channel directions. We consider three  $0.4 \mu\text{m} \times 0.2 \mu\text{m}$  2DEG channels along [100], [110], and [1 $\bar{1}$ 0], and inject an electron spin on the middle point of the left end. Without boundary effect, the injected spin is assumed to evolve freely to any position in the channel through a straight path. Using Eq. (1), we sketch the spin vectors of the injected electron, i.e., the expectation values of spin operators with respect to the injected electron state ket, as a function of position in Fig. 2. Here the influence due to the bulk inversion-asymmetry is clearly crucial, even in this Rashba dominating 2DEG. As suggested in our previous work,<sup>13</sup> channel directions should be chosen along [1 $\pm$ 10], in particular, along [110] due to stronger spin-splitting when  $\alpha\beta > 0$ , for better anticipation in the Datta-Das spin-FET. This is basically the fact that the

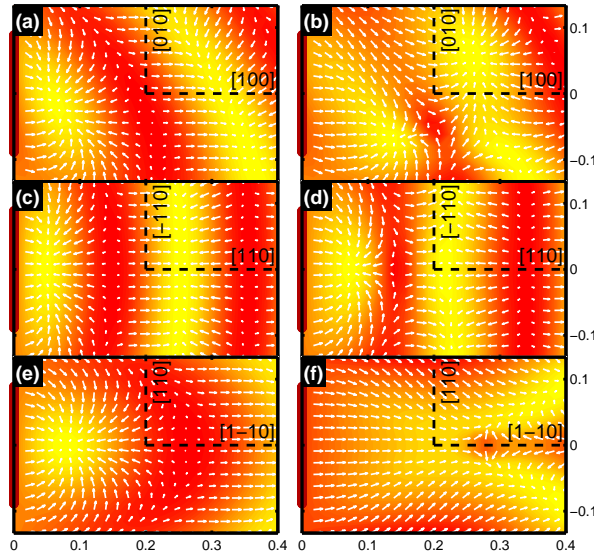


FIG. 3: (Color online) Spin vectors in  $0.4 \mu\text{m} \times 0.267 \mu\text{m}$  InGaAs 2DEGs with spin injection via finite-sized contacts (sketched by the bold dark lines on the left ends in each panel) with widths 2/3 times the channel width and polarization parallel to the channel direction. Left column (a), (c), and (e) are in the absence of the boundary effect while the right column (b), (d), and (f) considers the boundary effect.

Rashba and Dresselhaus terms generate an  $k$ -dependent effective magnetic field, which is perpendicular to the electron propagation only along  $\pm[1\pm 10]$ .

### B. Effects of finite-sized injection and channel boundary

We now consider  $0.4 \mu\text{m} \times 0.267 \mu\text{m}$  InGaAs 2DEG channels using finite-sized spin injection sources with side contacts. We set the width of the contact 2/3 times the channel width, and assume perfect polarization of the source contact in the spin transistor geometry. Again, we analyze cases with channel directions along [100], [110], and [1̄10], with and without the boundary effect. Based on the formalism we constructed in Secs. II B and II C, we plot the spin vectors in Fig. 3, where the left and right columns are in the absence and in the presence of the boundary effect, respectively. Compared to the single-point injection shown in Fig. 2, the variation due to the finite-sized spin injection seems tiny in the case without the boundary effect [Figs. 3(a), (c), and (e)], and the assumption of single-point injection may thus work well in this case. When the boundary effect is taken into account, the spin vectors are drastically changed, as can be clearly observed in Figs. 3(b), (d), and (f). Comparing (a), (c), and (e) with (b), (d), and (f), respectively, one can roughly conclude that the influence due to the boundary effect is inversely proportional to the SO strength, recalling that this spin-splitting is strongest along [110] whereas that along [1̄10] is weakest when  $\alpha$  and  $\beta$  are of the same sign. In fact, this is also true for the influence

due to the finite-sized injection, as will be clearer later.

To specify the change due to the finite-sized spin injection and the channel boundary effect, we now analyze  $\langle S_x \rangle$  along the straight paths in the middle of each channel, as shown in Fig. 4. Comparing the gray-dashed lines (finite-sized injection without boundary) with the black-solid lines (single-point injection without boundary), the effect of the finite-sized injection merely reduces the spin precession periods near the source contacts, as most obvious in the [1̄10] case [Fig. 4(c)], in which the SO strength is weakest. This may imply an effective enhancement of the spin-splitting due to a wide spin injection contact. In the strongest spin-splitting case [Fig. 4(b)], the two lines (black-solid and gray-dashed) nearly coincide and thus the assumption of the single-point injection works almost exactly. In the presence of the boundary effect, the behavior of the influence due to the finite-sized injection described above becomes even clearer, i.e., the difference between the single-point injection (the gray-solid lines) and the finite-sized injection (the black-dashed lines) is inversely proportional to the SO strength. In particular, the difference becomes drastic

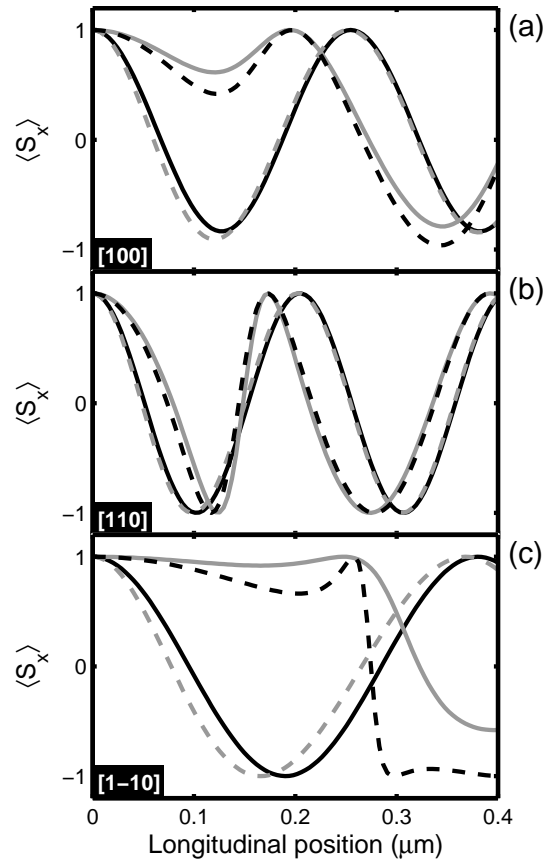


FIG. 4: The  $x$ -component of the spin vector  $\langle S_x \rangle$  along the straight path in the middle of a (a) [100], (b) [110], and (c) [1̄10] channel. Legend: black-solid and gray-dashed lines depict single-point and finite-sized injection cases, respectively, without the boundary effect; gray-solid and black-dashed lines depict single-point and finite-sized injection cases, respectively, in the presence of the boundary effect.

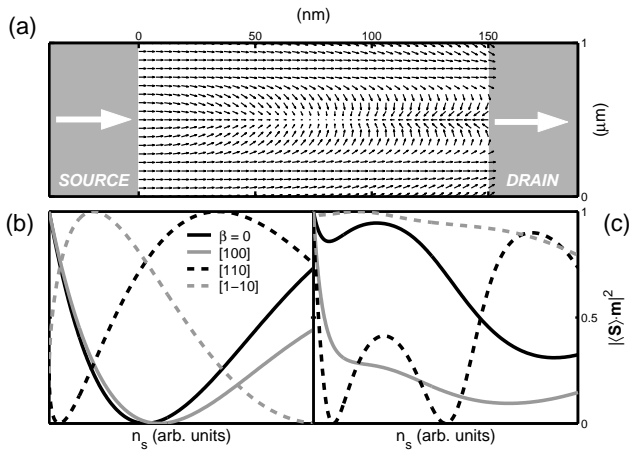


FIG. 5: (a) Spin vectors inside a  $150 \text{ nm} \times 1.0 \mu\text{m}$  Rashba-type 2DEG channel with ferromagnetic source and drain contacts in spin transistor geometry. The single-point injection is assumed with the injection point set on the middle of the source contact.  $|\langle \mathbf{S} \rangle \cdot \mathbf{m}|^2$  as a function of the carrier density  $n_s$  of the 2DEG, determined on the middle point at the end of the channel, (b) in the absence and (c) in the presence of the boundary effect. The unit vector of the drain magnetization  $\mathbf{m}$  is set parallel with the channel direction. The black-solid line corresponds to the pure Rashba system ( $\beta = 0$ ). The gray-solid, black-dashed, and gray-dashed lines are plotted in the presence of the Dresselhaus term with  $\beta = 0.09 \text{ eV Å}$ , along [100], [110], and [1-10], respectively. The ranging of the carrier density  $n_s$  correspond to  $\alpha = 0 - 0.22 \text{ eV Å}$ .

in the  $[1\bar{1}0]$  case [Fig. 4(c)].

We now focus on the effect due to the boundary reflection. Taking the single-point injection cases (black- and gray-solid lines) for illustration, we noticed again that the change due to the boundary effect also appears the most drastic in the case of  $[1\bar{1}0]$ , where the spin precession of the injected electron is almost destroyed. In these particular cases with channel width  $0.267 \mu\text{m}$ , one can roughly observe that the interference effects due to the boundary reflection occur within the region near  $0.15 \mu\text{m}$ . Also, the increase of the SO strength seems to squeeze the interference region [widest in 4(c) while narrowest in 4(b)]. When one considers wider (narrower) channels, the influence of the boundary effect becomes stronger (weaker). This also agrees with the previous suggestions of using quasi-one-dimensional channel for enhancing the performance of the Datta-Das transistor.<sup>16</sup> Further description of the boundary reflection effect may not be easily accessible since the interference of the straight propagating wave of the injected electron itself with the side-reflected waves is complicated.

### C. Datta-Das spin-FET

We finally make a simple connection to the ballistic method, solving for the transmission problem in a ferromagnet-2DEG-ferromagnet double junction structure,

constructed by Matsuyama *et al.*,<sup>18</sup> who considered only the Rashba term in the 2DEG channel. As shown in Fig. 5(a), we analyze the inplane components of the spin vectors in a  $150 \text{ nm} \times 1.0 \mu\text{m}$  Rashba-type 2DEG (for consistency with their work), using the method of single-point injection.

Whereas the ferromagnet and 2DEG regions are both spin-dependent, the electrons may transit between different spin subbands belonging to different regions. Based on the time-independent Schrödinger equation, one can obtain the corresponding transmission probabilities, which are found to depend on the Fermi velocity mismatch between the two regions and the spinor overlap between the incoming and outgoing states. Of particular interest is that the transmission probabilities (and, in fact, also the reflection probabilities) are proportional to this spinor overlap. Put in another way, the electron dislikes changing its spin when crossing the boundary between the ferromagnet and 2DEG regions. In this sense, one can clearly see why the oblique injections contribute an undesired background to the transmission probability, and hence the conductance,<sup>18</sup> by noting that the spin vectors at the end of the channel are nonuniform [Fig. 5(a)].

Focusing on the normal injection [center path in the channel of Fig. 5(a)], the spin vectors indeed precess upright down the way to the drain, as the original design of the Datta-Das spin-FET.<sup>1</sup> Using the relation<sup>18</sup>  $n_s \propto \alpha^2$ , we plot the squared norm of the spin vector along the magnetization direction  $|\langle \mathbf{S} \rangle \cdot \mathbf{m}|^2$ , which is responsible for the transmission probabilities  $T_{\pm,\pm}$ , as a function of the carrier density  $n_s$  with and without the boundary effect in Figs. 5(b) and (c), respectively. In the absence the boundary effect [Fig. 5(b)], the squared projection  $|\langle \mathbf{S} \rangle \cdot \mathbf{m}|^2$  is isotropic and shows no dependence on the crystallographic direction, when the Dresselhaus term is not involved. Despite the rapid oscillations caused by the Fabry-Perot interference between the source-2DEG and 2DEG-drain boundaries, we obtain a satisfactory curve [black-solid line in Fig. 5(b)], in good agreement of Ref.<sup>18</sup> [see Figs. 10(c) – (f) therein]. We again stress on the importance of choosing the channel direction for the Datta-Das transistor in the presence of the bulk-inversion-asymmetry (the Dresselhaus term), by noting that the precession behavior of the injected spin is sensitive to the channel direction [the other three lines in Fig. 5(b)]. As mentioned previously, a proper candidate is  $[110]$ , along which the bulk-inversion-asymmetry even enhances the SO strength, and hence the precession rate, without destroying the expected spin precession behavior in the Datta-Das spin-FET.

We end the discussion with Fig. 5(c), where the boundary effect is clearly observed, comparing with Fig. 5(b). In this case the spin precession behavior is drastically changed. As we have concluded previously that the spin vectors are less influenced by the boundary reflection for 2DEG channels along directions with stronger spin-splitting (e.g.,  $[110]$  case), the  $[110]$  curve [black-dashed line in Fig. 5(c)] is, however, also deteriorated. This is because the channel width is too wide, allowing a much severer influence caused by the boundary reflection. When the spin-orbit coupling strength, and hence the carrier density in this case, is strong enough, one can see that the precession behavior is recovered.

#### IV. CONCLUSION

We have completed the analytical formulae for the spin vectors, i.e., the spin expectation values done with respect to the injected electron spin state, in inversion-asymmetric 2DEGs with both the Rashba and Dresselhaus terms involved. The derived formulae are applicable for arbitrarily polarized spin injected via an ideal point contact. In this case one can see that the injected spin with polarization parallel to the channel direction precesses upright only along  $\pm[1\pm 10]$ , which are therefore candidates for the Datta-Das spin-FET channel directions.

By straightforward extension to the finite-sized spin injection case, we have demonstrated that the size of the source contact does not play a decisive role in the detection of the injected spin. In fact, the influence, which is found to be inversely proportional to the SO strength, becomes obvious only in regions near the source contact, and the analysis within the framework of the single-point spin injection works well. Detailed comparison (Fig. 4) has even shown that the average effect of the finite-sized injection is to provide a slight enhancement of the spin-splitting. We also noticed that when considering a top contact of spin injection, the calculated spin vectors are not sensitive to the crystalline structure of the source contact. For example, using a bcc Fe contact or a hexagonal Co contact with the same shape and size does not show any primary difference in our model of finite-sized spin injection.

We also proposed a simple model to test the effect of the channel boundary. Treating the space part of the wave function of an electron injected into the 2DEG as plane waves, we considered the side boundaries of the channel as perfectly flat, so that the electron plane waves may encounter usual reflections, leading to certain interferences. Such interferences are found to be of crucial effects on the spin vectors. Comparing with [100], [110], and [110] channel directions, the influences caused by the boundary reflection seem to be, again, inversely proportional to the strength of the spin-splitting. The spin precession behaviors are drastically destroyed by the boundary reflection, and even more deteriorated when the channel width is wide, comparing the distance between the source contact

and the detection point.

We finally took Ref.<sup>18</sup> as an example for illustrating the significance of the channel direction when both the Rashba and Dresselhaus terms are involved, and the influence due to the boundary reflection. In the sense that the transmission probabilities are proportional to the projection of the incoming spin state to the outgoing one, we have showed that our results can be connected to Ref.<sup>18</sup>. Whereas the channel width in this case is much longer than the channel length, the boundary reflection almost completely destroys the original spin precession behavior.

We emphasize here the two-dimensional wave property of the electron in typical InGaAs 2DEGs. From degenerate perturbation theory, one is led to the criterion<sup>1,16</sup>  $W \ll \hbar^2/\alpha m^*$ , within which the channel can be regarded as quasi-one-dimensional, when assuming hard wall lateral confinement and considering only the Rashba term. For the Rashba-Dresselhaus 2DEGs with, e.g.,  $\alpha = 0.3 \text{ eV \AA}$ ,  $\beta = 0.09 \text{ eV \AA}$ , and  $m^* = 0.03m_e$ , considered in Secs. III A and III B, the total coupling strength ranges from  $0.21 \text{ eV \AA}$  (the  $[1\bar{1}0]$  direction) to  $0.39 \text{ eV \AA}$  (the  $[110]$  direction). The criterion for the quasi-one-dimensional channel will require  $W \ll 65 \text{ nm}$  ( $121 \text{ nm}$ ) for the  $[110]$  ( $[1\bar{1}0]$ ) case. Therefore, typical InGaAs 2DEGs with channel widths of the order of or larger than these lengths will require two-dimensional description for the electron waves, and the possible boundary effects are thus unavoidable.

Our results may be taken as a warning indicating another difficulty inherent in the design of Datta-Das spin-FET: the interference due to the side boundaries. However, we conclude that the  $[110]$  direction is shown to be robust under the influence of finite-sized spin injection and the boundary reflection, for [001]-grown zincblend-based 2DEGs.

#### Acknowledgments

This work was supported by the Republic of China National Science Council Grant No. 93-2112-M-002-011.

<sup>1</sup> S. Datta and B. Das, *Appl. Phys. Lett.* **56**, 665 (1990).

<sup>2</sup> *Semiconductor Spintronics and Quantum Computation*, edited by D. D. Awschalom, D. Loss, and N. Samarth (Springer, Berlin, 2002).

<sup>3</sup> Igor Žutić, Jaroslav Fabian, and S. Das Sarma, *Rev. Mod. Phys.* **76**, 323 (2004).

<sup>4</sup> E. I. Rashba, *Sov. Phys. Solid State* **2**, 1109 (1960); Yu. A. Bychkov and E. I. Rashba, *JETP Lett.* **39**, 78 (1984).

<sup>5</sup> B. Jusserand, D. Richards, G. Allan, C. Priester, and B. Etienne, *Phys. Rev. B* **51**, R4707 (1995);

<sup>6</sup> W. Knap, C. Skierbiszewski, A. Zduniak, E. Litwin-Staszewska, D. Bertho, F. Kobbi, J. L. Robert, G. E. Pikus, F. G. Pikus, S. V. Iordanskii, V. Mosser, K. Zekentes, and Yu. B. Lyanda-Geller, *Phys. Rev. B* **53**, 3912 (1996); J. B. Miller, D. M. Zumbühl, C. M. Marcus, Y. B. Lyanda-Geller, D. Goldhaber-Gordon, K. Camp-

man, and A. C. Gossard, *Phys. Rev. Lett.* **90**, 076807 (2003); S. D. Ganichev, V. V. Bel'kov, L. E. Golub, E. L. Ivchenko, P. Schneider, S. Giglberger, J. Eroms, J. De Boeck, G. Borghs, W. Wegscheider, D. Weiss, and W. Prettl, *Phys. Rev. Lett.* **92**, 256601 (2004).

<sup>7</sup> J.M. Kikkawa and D.D. Awschalom, *Phys. Rev. Lett.* **80**, 4313 (1998).

<sup>8</sup> J. Nitta, T. Akazaki, H. Takayanagi, and T. Enoki, *Phys. Rev. Lett.* **78**, 1335 (1997).

<sup>9</sup> G. Dresselhaus, *Phys. Rev.* **100**, 580 (1955).

<sup>10</sup> A. Łusakowski, J. Wróbel, and T. Dietl, *Phys. Rev. B* **68**, R081201 (2003).

<sup>11</sup> R. Winkler, *Spin-Orbit Coupling Effects in Two-Dimensional Electron and Hole Systems* (Springer, Berlin, 2003).

<sup>12</sup> R. Winkler, *Phys. Rev. B* **69**, 045317 (2004).

<sup>13</sup> Ming-Hao Liu, Ching-Ray Chang, and Son-Hsien Chen, Phys. Rev. B **71**, 153305 (2005).

<sup>14</sup> J. Kainz, U. Rössler, and R. Winkler, Phys. Rev. B **68**, 075322 (2003).

<sup>15</sup> J. J. Sakurai, *Modern Quantum Mechanics* Rev. ed. (Addison-Wesley, 1994).

<sup>16</sup> F. Mireles and G. Kirczenow, Phys. Rev. B **64**, 024426 (2001).

<sup>17</sup> Jun Wang, H. B. Sun, and D. Y. Xing, Phys. Rev. B **69**, 085394 (2004)

<sup>18</sup> T. Matsuyama, C.-M. Hu, D. Grundler, G. Meier, and U. Merkt, Phys. Rev. B **65**, 155322 (2002).

<sup>19</sup> Y. Sato, T. Kita, S. Gozu, and S. Yamada, J. Appl. Phys. **89**, 8017 (2001).

<sup>20</sup> G. Lommer, F. Malcher, and U. Rössler, Phys. Rev. Lett. **60**, 728 (1988); B. Jusserand, D. Richards, H. Peric, and B. Etienne, Phys. Rev. Lett. **69**, 848 (1992).